

1 **Combined effects of polystyrene microplastics and thermal**  
2 **stress on the freshwater mussel *Dreissena polymorpha***

3  
4 ***Supplementary Information***

5  
6 Annkatriin Weber<sup>a\*</sup>, Nina Jeckel<sup>a\*</sup>, Martin Wagner<sup>b</sup>

7 <sup>a</sup> Goethe University Frankfurt am Main, Department of Aquatic Ecotoxicology, Max-von-Laue-  
8 Straße 13, 60438 Frankfurt am Main, Germany

9 <sup>b</sup> Norwegian University of Science and Technology, Department of Biology, Høgskoleringen  
10 5, Realfagbygget, 7491 Trondheim, Norway

11  
12 \*Both authors contributed equally to this work.

---

13  
14 Corresponding author's contact details: Martin Wagner, martin.wagner@ntnu.no

15

## 16 **S1 Supplementary materials and methods**

### 17 ***S1.1 Particle preparation***

18 Microplastics (MP) were produced by cryomilling in a swing mill (Retsch, MM400, Haan,  
19 Germany) with a stainless-steel milling chamber (volume: 50 mL, Retsch Technology, Haan,  
20 Germany) and a Ø 25 mm stainless steel ball. The polystyrene (PS) cup was crushed into  
21 pieces of up to 3 cm length and 5 g of these pieces were ground three times for 4 min at 30 Hz.  
22 Before and between the runs, the chamber was cooled with liquid nitrogen for 2 min.

23 300 g of MP and diatomite (DI) powder were separately sieved through a 63 µm woven wire  
24 mesh sieve (Retsch, product no.: 60.131.000063, Haan, Germany) on a sieving tower (Retsch  
25 Technology, AS200basic, Haan, Germany) for 4 h (amplitude: 20 Hz).

26

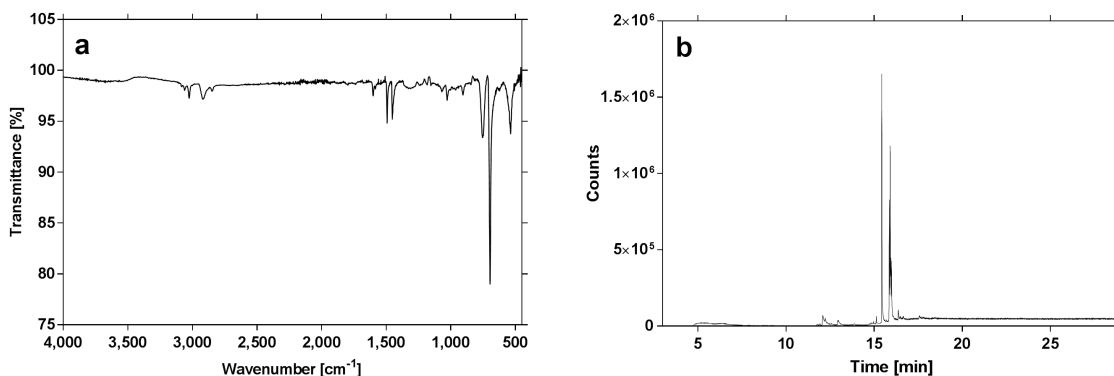
### 27 ***S1.2 Particle characterization***

28 PS as polymer type was verified by Fourier-transform infrared spectroscopy in Attenuated  
29 Total Reflection mode (ATR-FTIR spectroscopy, Spectrum 2, Perkin Elmer, Waltham, MA,  
30 USA). The polymer spectrum was measured with the range set to 4,000–450 cm<sup>-1</sup> (4 scans  
31 per wave number, resolution: 4 cm<sup>-1</sup>, suppression of CO<sub>2</sub> and H<sub>2</sub>O peaks). The major peaks in  
32 the FTIR spectrum (Fig. S1a) were in accordance with the data published by Jung et al. (2018)  
33 and confirmed that the material was PS.

34

35 The chemical content in the PS sample was determined by pyrolysis-GC-MS (py-GC-MS,  
36 Multi-Shot Pyrolyzer and Auto-Shot Sampler (Frontier Laboratories, Saikon, Japan) attached  
37 to an Agilent 7890B gas chromatograph and an Agilent 5977B Mass Selective Detector  
38 (Agilent, Santa Clara, CA, USA)). PS powder (100–300 mg per pyrolysis cup) was heated to  
39 280 °C for 5 min. Thermodesorption products were detected for 30 min in selected ion  
40 monitoring mode.

41



42

43 Fig. S1: (a) ATR-FTIR spectrum and (b) py-GC-MS spectrum of the polystyrene drinking cups.

44 The py-GC-MS spectrum (Fig. S1b) was analyzed with the Agilent MassHunter Workstation  
 45 Software (version B.05.00, Agilent Technologies, Santa Clara, CA, USA) using  
 46 “Chromatogram Deconvolution”. We only analyzed peaks with an absolute height of at least  
 47 2 % of the highest peak and with a relative height of at least 5,000 counts. Additional settings  
 48 were: RT window size factor = 100, peak filter = excluded m/z: 28, extraction window: left m/z  
 49 delta = 0.3 and right m/z delta = 0.7. The mass spectra of the resulting peaks were compared  
 50 to the NIST 2011 Mass Spectral Library (National Institute of Standards and Technology,  
 51 Gaithersburg, MD, USA).

52 We detected the fluorophore 1,4-diphenyl-,(E,E)-1,3-butadiene, (Tab. S1) as well as  
 53 m-phenethyl-benzonitrile, and (2,3-Diphenylcyclopropyl)methyl phenyl sulfoxide as  
 54 thermodesorption products. The fluorophore might originate from the dye of the drinking cup.  
 55 The other two desorption products, however, are not commonly used in polymers and their  
 56 origin, therefore, remains unknown.

57 Tab. S1: Detected peaks in the py-GC-MS mass spectrum and corresponding tentative identification based on the  
 58 NIST database (highest match scores).

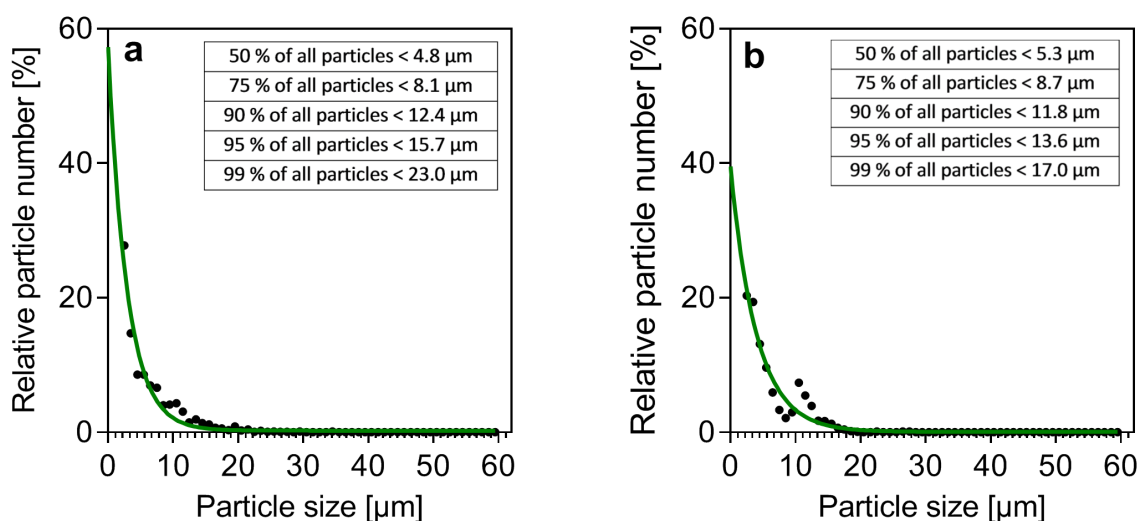
	Polymer	Base Peak	RT	Height	Area	Compound name	Score
1	PS	90.99	12.089	21,601	245,656	not identified	none
2	PS	104.01	12.223	14,719	85,223	not identified	none
3	PS	204.02	12.947	6,699	66,710	not identified	none
4	PS	90.99	15.430	622,777	2,067,796	Benzonitrile, m-phenethyl-	57.03
5	PS	90.99	15.856	156,943	1,009,078	1,3-Butadiene, 1,4-diphenyl-, (E,E)-	73.09
6	PS	90.99	15.904	233,782	1,639,405	(2,3-Diphenylcyclopropyl)methyl phenyl sulfoxide, trans-	75.13
7	PS	90.99	15.942	83,831	477,232	(2,3-Diphenylcyclopropyl)methyl phenyl sulfoxide, trans-	59.17
8	PS	90.99	15.983	84,599	781,256	(2,3-Diphenylcyclopropyl)methyl phenyl sulfoxide, trans-	67.09
9	PS	90.99	16.364	14,536	65,237	not identified	none
10	PS	90.99	16.485	6,457	98,021	not identified	none

59

### 60 **S1.3 Particle concentrations and size distribution**

61 The concentrations of MP and DI particles ( $\leq 63 \mu\text{m}$ ) were determined using a Coulter Counter  
62 (Beckman Coulter, Multisizer 3, Krefeld, Germany) by suspending 2 mg MP or DI in 50 mL  
63 electrolytic solution (0.9 % NaCl solution,  $< 0.2 \mu\text{m}$  sterile-filtered) and adding 5 mL of these  
64 suspensions to 147 mL electrolytic solution. The suspension was directly measured three  
65 times with a  $100 \mu\text{m}$  capillary (Beckman Coulter, Krefeld, Germany, detection range: 2–60  $\mu\text{m}$ ,  
66 aperture: -1,600, gain: 2, analytical volume: 1 mL). The measurements were repeated three  
67 times for both particle types. Additionally, background measurements without MP or DI were  
68 performed to quantify contamination in the electrolyte solution. The MP and DI concentrations  
69 were corrected, accordingly. The MP and the DI powder contained  $287,526 \text{ particles per mg}^{-1}$   
70 and  $4,632,990 \text{ particles mg}^{-1}$ , respectively.

71 Results on particle size distributions from Coulter Counter measurements were averaged and  
72 fitted with GraphPad-Prism Software (Version 7.04, San Diego, CA) using a “One phase  
73 decay” function (relative particle size, Fig. S2) or a “One phase association” function  
74 (cumulative particle size of MP) and a “Cumulative Gaussian-Percentage” function (cumulative  
75 particle size of DI). From the cumulative size distributions, we determined the maximum size  
76 of 50, 75, 90, 95 and 99 % of the particles (insets in Fig. S2).



77

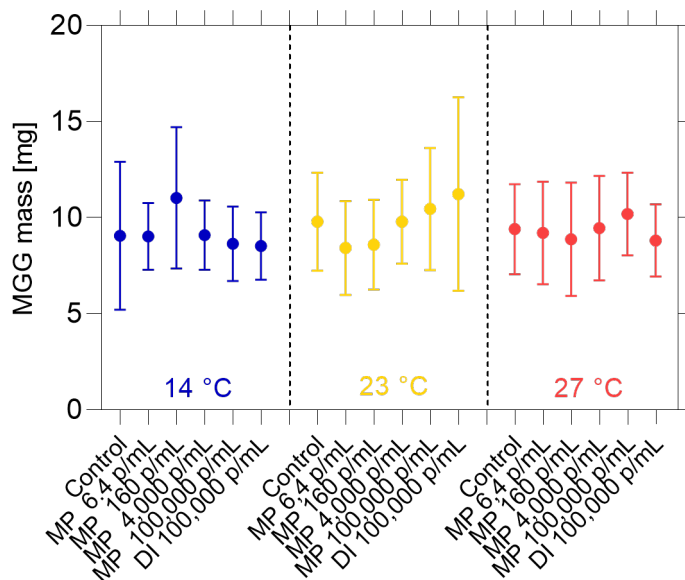
78 Fig. S2: Relative size distribution of (a) microplastics and (b) diatomite particles. Size distribution was summarized  
79 from three separate measurements and approximated with a One phase decay function using GraphPad Prism.  
80 The tables in the insets present the results derived from cumulative particle distributions.

81

82

### 83 **S1.4 Preparation of midgut gland homogenates**

84 Midgut glands (MGG) from ten individuals per treatment were dissected and weighed. Fig. S3  
85 indicates that MGG mass varied intensively within each exposure group, while MGG mass did  
86 not differ significantly between any of the exposure groups (Kruskal-Wallis test,  $p > 0.05$ ).



87  
88 Fig. S3: Midgut gland mass (MGG, mean  $\pm$  standard deviation) of *D. polymorpha* after an exposure to particle-free  
89 medium (Control, 0 p mL<sup>-1</sup>), polystyrene microplastics (MP, 6.4–100,000 p mL<sup>-1</sup>) or diatomite (DI, 100,000 p mL<sup>-1</sup>)  
90 for 14 d at 14, 23 and 27 °C.

91

92 Midgut glands (MGG) were homogenized in 360  $\mu$ L of potassium phosphate buffer (PPB;  
93 10 mM, pH 7.4) with two stainless steel balls ( $\varnothing$  2–3 mm) in a swinging mill for 30 min  
94 (15 $\times$ 2 min). The tissue as well as its homogenate was constantly placed on ice between the  
95 processing steps to avoid degradation.

96 For the glycogen and total lipid assay, 150  $\mu$ L of midgut gland homogenate was mixed with  
97 50  $\mu$ L 2 % (m/v) Na<sub>2</sub>SO<sub>4</sub> solution (Sigma-Aldrich, Munich, Germany). 25  $\mu$ L of this mixture was  
98 further diluted with 6.25  $\mu$ L 2 % Na<sub>2</sub>SO<sub>4</sub> solution and 18.75  $\mu$ L PPB to obtain the required  
99 dilution for the protein assay.

100 For the thiobarbituric reactive substances assay (TBARS), 160  $\mu$ L of each tissue homogenate  
101 were mixed with 160  $\mu$ L PPB (10 mM, pH 7.4). The dilution for the oxygen radical absorbance  
102 capacity assay (ORAC) was produced by mixing 10  $\mu$ L of the TBARS dilution with 90  $\mu$ L PPB.

103

### 104 **S1.5 Protein, glycogen and total lipid assay**

105 S1.5.1 Protein assay

106 The protein assay was performed according to Bradford (1976). As standard, 1, 3, 6, 12.5, 25,  
107 37.5 and 50  $\mu\text{L}$  of a 0.1 % (m/v) bovine serum albumin solution (BSA; Sigma-Aldrich,  
108 Darmstadt, Germany) were mixed with 2 %  $\text{Na}_2\text{SO}_4$  solution to obtain a total volume of 50  $\mu\text{L}$ .  
109 50  $\mu\text{L}$  of 2 %  $\text{Na}_2\text{SO}_4$  solution were used as negative control. The negative control, the  
110 standards as well as 50  $\mu\text{L}$  of the homogenate dilution (see S1.4) were mixed with 1.5 mL  
111 Bradford reagent (A6932, AppliChem GmbH, Darmstadt, Germany) and incubated for 5 min at  
112 room temperature. Subsequently,  $2 \times 200 \mu\text{L}$  were pipetted into transparent 96-well plates and  
113 optical density was determined spectrometrically at 595 nm (Spark 10, Tecan, Switzerland).

114 S1.5.2 Glycogen and total lipid assay

115 100  $\mu\text{L}$  of homogenate dilution for the glycogen and total lipid analysis (S1.8) were mixed with  
116 1.6 mL of a 1:1 chloroform-methanol solution (chloroform: VWR International, Darmstadt,  
117 Germany; methanol: Carl Roth, Karlsruhe, Germany). After 1 h of incubation on ice,  
118 homogenates were centrifuged at 845 g for 2 min (Centrifuge 5702, Eppendorf, Hamburg,  
119 Germany). The pellet was analysed for its glycogen content, while the supernatant (which  
120 includes the lipid fraction) was separated, mixed with 600  $\mu\text{L}$  distilled water and centrifuged at  
121 845 g for 2 min. Subsequently, the resulting upper phase was removed, and the lower phase  
122 was used for total lipid analysis.

123 For glycogen analysis, the pellet was dissolved in 5 mL of anthrone-sulphuric acid reagent  
124 (750 mg anthrone, Merck, Darmstadt, Germany; 385 mL 98 %  $\text{H}_2\text{SO}_4$ , VWR, Darmstadt,  
125 Germany; 150 mL demineralized water) and incubated in a water bath at 95 °C for 17 min. As  
126 standard, 1, 3, 6, 12.5, 25, 50, 100, 200, 400 and 800  $\mu\text{L}$  of a 0.1 % (m/v) D-(+)-glucose  
127 solution (VWR, Darmstadt, Germany) was processed in the same way. As negative control,  
128 5 mL of anthrone-sulphuric acid reagent were incubated alone.  $2 \times 200 \mu\text{L}$  from each replicate  
129 were pipetted into transparent 96-well plates and optical density was determined  
130 spectrometrically at 625 nm.

131 Lipid fractions were reduced to a volume of approximately 20  $\mu\text{L}$  by evaporation in a water  
132 bath at 70 °C. As standard, 1, 3, 6, 12.5, 25, 50, 100, 200, 400 and 800  $\mu\text{L}$  of a canola oil  
133 solution (0.1 % v/v in chloroform, REWE, Cologne, Germany) were concentrated in the same  
134 way. Then, 200  $\mu\text{L}$  of sulphuric acid (95–98 %, CAS: 7664-93-9, VWR, Darmstadt, Germany)  
135 were added and samples were incubated in the water bath at 70 °C for 13 min. As negative  
136 control, 200  $\mu\text{L}$  of sulphuric acid were incubated alone. After the incubation, 5 mL of vanillin-  
137 phosphoric acid reagent (600 mg vanillin, Sigma-Aldrich, Munich, Germany; 400 mL 85 %  
138  $\text{H}_3\text{PO}_4$ , VWR, Darmstadt, Germany, 100 mL demineralized water) were added to all samples

139 and incubated at room temperature for 5 min. Finally, 2×200 µL from each tube were  
140 transferred into a transparent 96-well plate and the absorbance was recorded at 560 nm using  
141 a Tecan Spark 10 photospectrometer.

### 142 S1.5.3 Calculation of the energy content

143 Protein, glycogen and total lipid contents were determined by plotting the optical densities of  
144 the BSA, glucose and canola oil standard solutions as a function of its energy content [µg].  
145 Energy values were estimated as 17.2 J mg<sup>-1</sup> for proteins and glucose (Higgs et al. 1995) as  
146 well as 34.04 J mg<sup>-1</sup> for lipids (REWE, product information) and recalculated for each standard  
147 dilution. The energy contents of the MGG samples were interpolated from a quadratic  
148 regression of the results from the standard measurements and normalized to the MGG wet  
149 weight [J mg<sup>-1</sup>]. Finally, we calculated individual protein, glycogen and total lipid contents in the  
150 MGG as well as the total energy content (= energy content of proteins+glycogen+total lipids).

151

## 152 **S1.6 Oxidative stress assays**

### 153 S1.6.1 Thiobarbituric acid assay (TBARS)

154 Malondialdehyde (MDA) as standard substance was produced by hydrolysis of 1,1,3,3-  
155 Tetramethoxypropane (TMP, Sigma-Aldrich, Munich, Germany). 41.2 µL of TMP were added  
156 to 250 mL ultrapure water and 0.25 mL hydrochloric acid (1 M, CAS: 7647-01-0, VWR,  
157 Darmstadt, Germany) and incubated at 52–55 °C in a heating cabinet for at least 1 h through  
158 which a 1 mM aqueous solution was produced. A serial dilution (80, 40, 20, 10, 5, 2.5 µM) of  
159 the MDA solution was prepared as standard. Ultrapure water was used as negative control.

160 100 µL of the homogenate dilutions (S1.4, two replicates per homogenate), of the negative  
161 control (three replicates) as well as of the MDA standard (three replicates per concentration)  
162 were mixed with 100 µL of an ice-cold 10 % (m/v) trichloroacetic acid solution and 120 µL of a  
163 2 mM thiobarbituric acid solution (Sigma-Aldrich, Munich, Germany). The mixture was  
164 incubated at 95 °C for 1 h and, after cooling down to room temperature, mixed with 180 µL  
165 butanol-pyridine-mixture (14:1 ratio; 1-butanol: AppliChem, Darmstadt, Germany; pyridine:  
166 Sigma-Aldrich, Munich, Germany). Samples were centrifuged at 5,200 g and 0 °C for 5 min for  
167 phase separation. Subsequently, 80 µL of the upper phase were pipetted into black 96-well  
168 plates (Nunc F96 MicroWell, Thermo Fisher Scientific, Waltham, USA) and fluorescence was  
169 measured (extinction: 540 nm, emission: 590 nm, gain: 48) using a Tecan Spark 10  
170 spectrophotometer. Fluorescence of the replicate samples (see above) was averaged.

171 We determined lipid peroxidation in the MGG by comparing the fluorescence of samples with  
172 the fluorescence of the MDA standard. For this, results of the MDA standard and the negative  
173 control were plotted as a quadratic function of the concentration and MDA equivalents in the  
174 MGG samples were interpolated from this function. Due to high variability of total lipid contents  
175 in the different treatments, we chose to normalize the resulting MDA equivalents to MGG wet  
176 weight ( $\mu\text{mol mg}^{-1}$ ) and not to the total lipid content.

### 177 S1.6.2 Oxygen radical absorbance capacity assay (ORAC)

178 For each ORAC assay, a standard was produced from a 200  $\mu\text{M}$  6-hydroxy-2,5,7,8-  
179 tetramethylchroman-2-carboxylic acid (Trolox) solution (Sigma-Aldrich, Munich, Germany) by  
180 dilution (200, 100, 50, 25, 12.5, 6.25  $\mu\text{mol}$ ). PPB was used as negative control.

181 20  $\mu\text{L}$  of the control (three replicates), of the homogenate dilutions (S1.4, two replicates per  
182 homogenate) as well as of the Trolox standard (three replicates per concentration) were  
183 pipetted into a black 96-well plates. 150  $\mu\text{L}$  of a 0.106  $\mu\text{M}$  fluorescein solution (Sigma-Aldrich,  
184 Munich, Germany) was added to each well and plates were incubated at 37 °C for 20 min.  
185 Finally, 30  $\mu\text{L}$  of a 152.66 mM 2,2'-azobis (2-methylpropionamidine) dihydrochloride solution  
186 (AAPH, Sigma-Aldrich, Munich, Germany) were quickly added to each well and fluorescence  
187 (extinction: 485 nm, emission: 520 nm, gain: 43) was recorded at 37 °C in 1 min intervals for  
188 12 h on a Tecan Spark 10 instrument.

189 For data analysis, fluorescence values of the Trolox standard and the analysed samples were  
190 plotted as a function of the measurement time (12 h) and the area under each curve (AUC)  
191 was determined for each sample. AUC results of replicates were expressed as means. AUC  
192 values of the Trolox standard were plotted as a function of the concentration and the  
193 antioxidative capacity of the homogenates were interpolated as Trolox equivalents.  
194 Correspondingly to the TBARS assay, we normalised the antioxidative capacity to the MGG  
195 wet weight ( $\mu\text{mol mg}^{-1}$ ).

196

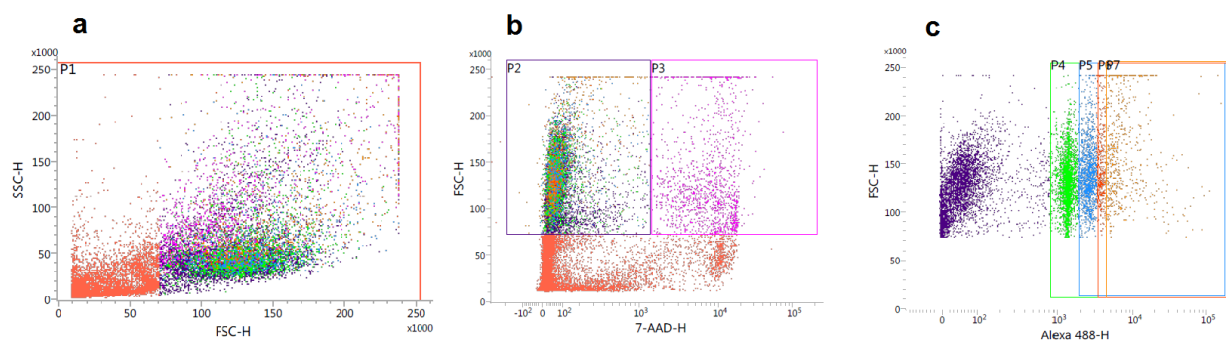
### 197 **S1.7 Phagocytic activity of *D. polymorpha* hemocytes**

198 For analysis of hemocyte phagocytic activity, we extracted 250–300  $\mu\text{L}$  hemolymph from five  
199 mussels per treatment and immediately stored it in separate reaction tubes on ice. Hemocyte  
200 concentrations in the hemolymph were determined with a Neubauer improved counting  
201 chamber using trypan blue staining. Then, each hemolymph sample was diluted with  
202 *D. polymorpha* serum to a total volume of 500  $\mu\text{L}$  and a concentration of 300,000 cells  $\text{mL}^{-1}$ .  
203 *D. polymorpha* serum was produced by pooling hemolymph extracted from non-exposed



204 individuals and directly heating it to 56 °C for at least 30 min. After centrifugation at 21,130 g  
 205 for 15 min, the supernatant was directly frozen and later used as serum. 1 µm PS spheres  
 206 (Fluoresbrite YG microspheres, PolyScience, Hirschberg an der Bergstraße, Germany,  
 207 excitation: 441 nm, emission: 486 nm) suspended in *D. polymorpha* serum were added at a  
 208 ratio of 50 spheres per hemocyte cell (7.5 µL of a 10<sup>9</sup> spheres mL<sup>-1</sup> stock solution) to the  
 209 hemolymph. Each sample was gently vortexed and directly split in two subsamples with 250 µL  
 210 each, one being incubated at room temperature and the other one on ice.

211 After 3 h of incubation, 10 µg mL<sup>-1</sup> propidium iodide (PI, Sigma-Aldrich/Merck, Taufkirchen,  
 212 Germany, excitation: 482 nm, emission: 608 nm) were added and samples were directly  
 213 analysed using a BD FACSVerse (BD Biosciences, Heidelberg, Germany). PI penetrates the  
 214 membrane of dead cells and intercalates with nucleic acids. After excluding dead cells from  
 215 the main cell population according to PI fluorescence (Fig. S4a–b, Gate P2: living hemocytes  
 216 in the main cell population; Gate P3: dead hemocytes in the main cell population), we  
 217 determined the number of living hemocytes with ≥ 3 spheres (Gate P6 in Fig. S4c, Gate P6 is  
 218 a subpopulation from Gate P2). Only FACS analyses with ≥ 5,000 living cell counts were used.  
 219 We extrapolated data from all FACS measurements to 10,000 living cells to allow data  
 220 comparability between the different samples. Results from the sample exposed at room  
 221 temperature were corrected for the number of hemocytes with ≥ 3 spheres from sample  
 222 exposed on ice to account for particles which were adsorbed on the hemocytes cell surface,  
 223 but not phagocytized. Based on the corrected data, we determined the fraction of living  
 224 hemocytes with ≥ 3 spheres compared to all analyzed living hemocytes.



225

226 Fig. S4: Characterization of hemocytes exposed to 1 µm polystyrene spheres with FACSVerse. (a) Size (FSC) vs.  
 227 granularity (SSC) of analyzed hemocytes (488 nm laser, FSC: 254.6 Voltage, SSC (filter: 481-496 nm):  
 228 324.5 Voltage), (b) Gating of living (gate P2) and dead (gate P3) hemocytes due to PI fluorescence (488 nm laser,  
 229 7-AAD (filter: 673-727, mirror: 665 LP), 300.3 Voltage), (c) Gating of living hemocytes (from Gate 2) with ≥ 1 (P4),  
 230 ≥ 2 (P5), ≥ 3 (P6) or ≥ 4 spheres (P7) (488 nm laser, Alexa 488 (filter: 511-543, mirror: 507 LP), 304.5 Voltage).

231

## 232 **S1.8 Clearance rate of *D. polymorpha***

233 Clearance activity of *D. polymorpha* was assessed by exposing mussels individually to an  
234 algae suspension (*Pseudokirchneriella subcapitata*, 5,000–5,500 relative fluorescence units  
235 (RFUs), approximately  $1.48\text{--}1.64 \times 10^6$  cells mL<sup>-1</sup>) and measuring chlorophyll fluorescence prior  
236 to and after the exposure (emission: 440 nm, extinction: 680 nm, GENios, Tecan, Männedorf,  
237 Switzerland). 250 mL glass jars were filled with 50 mL algae suspension and gently stirred with  
238 a magnetic stirrer. Ten *D. polymorpha* individuals were randomly selected from each of the  
239 treatments and individually exposed to the algae suspension for 45 min (beginning from the  
240 time when the mussel opened its valves). Before the introduction of the mussels as well as  
241 after 45 min, 3×200 µL of algae suspension were removed from each exposure vessel and  
242 transferred into black 96-well plates. Algae concentrations were determined using chlorophyll  
243 fluorescence (RFU). OECD medium (OECD 2016, guideline no. 242) was used as blank  
244 sample to account for background fluorescence. Replicate results were expressed as means  
245 and the clearance rate of each *D. polymorpha* individual was expressed as  $\Delta\text{RFU} = \text{RFU}$   
246 (prior to exposure) – RFU (after exposure).

## 247 **S1.9 Statistics**

248 For clearance rate, energy reserves, oxidative stress and immunological results, we ran  
249 separate general linear models (GLM) with IBM SPSS (version 25) to determine the  
250 contribution of the variables “temperature“, “MP “ as well as their interaction on the overall  
251 effect. We included temperature (14, 23, 27 °C) as fixed variable and MP (0–100,000 p mL<sup>-1</sup>)  
252 as covariable in the model. In the GLM for the clearance rate, the variable MP obtained only  
253 two states (Control, 100,000 p mL<sup>-1</sup> MP) and MP was, therefore, also considered a fixed  
254 variable. For mussel activity, we analyzed the data from the six consecutive observation with  
255 a general linear mixed model (GLMM) with “time“ as inner-subject variable and “temperature“  
256 and “MP“ as between-subject variables.

257

258 Data for each endpoint was used as dependent variable and was either integrated  
259 untransformed (glycogen, clearance rate), log-transformed (protein, TBARS, ORAC), square-  
260 root transformed (total energy, total lipids) or logit-transformed (immunity, mussel activity) into  
261 the model. Normality (Shapiro-Wilks test), variance homogeneity (Levene test) and  
262 heteroskedasticity (White test) requirements were met for most data sets. In case of the GLMs  
263 for the ORAC and the immune assay results, outliers caused non-Gaussian distribution and  
264 heterogenic variances, respectively. In case of the GLM for the ORAC results, outlier removal  
265 did not lead to different results indicating robustness of the GLM, while for the immune function  
266 GLM the interaction term turned significant. In the results section, however, we present the  
267 more conservative results including the outlier to avoid overinterpretation of data.

268

269 We initially included the temperature  $\times$  MP interaction term in all GLMs. In case of a non-  
270 significant interaction term, we refined GLMs excluding the interaction terms. Results,  
271 however, did not differ and we, therefore, present the final results including the interaction term  
272 (except for the glycogen GLM where the interaction term is left out).

273

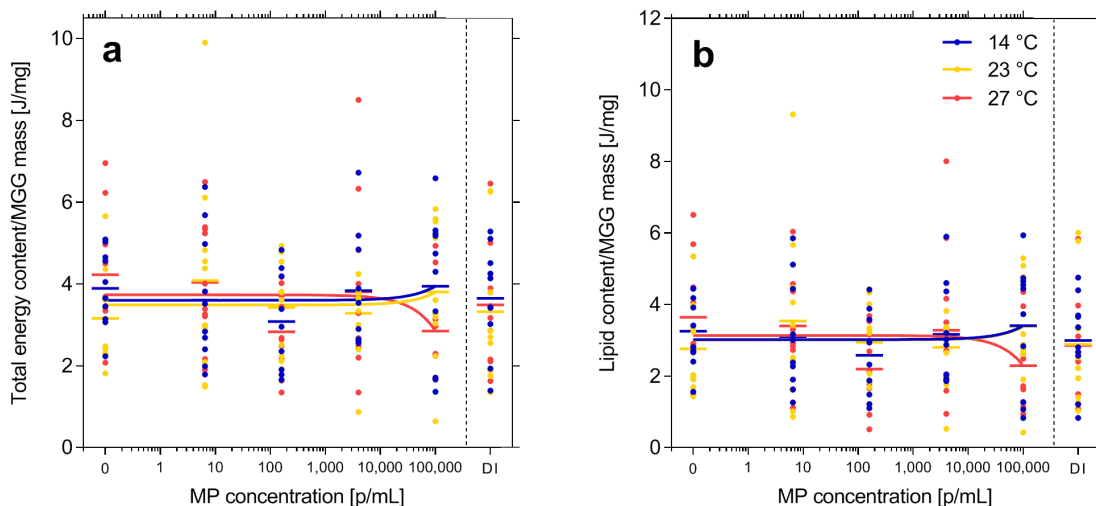
274 Statistic analysis of particle type effects (MP vs. DI) were performed in the same way as for  
275 MP effects. We ran GLM and GLMM with the variables “temperature“, “particle type“ (both fixed  
276 variables) and its interaction (temperature  $\times$  particle type) as well as “time“ as inner-subject  
277 variable in case of the GLMM for mussel activity. In case of the GLMM, the number of degrees  
278 of freedom were too low to integrate the interaction term into the model.

279 Dependent variable data was included untransformed (total energy, glycogen, total lipids,  
280 TBARS, ORAC, clearance rate), square root-transformed (protein) or logit-transformed  
281 (immunity, mussel activity) into the separate models. Normality, variance homogeneity and  
282 heteroskedasticity criteria were met for all data sets except for the clearance rate at day 3.  
283 Data on clearance rates was non-normally distributed according Shapiro-Wilks test, but visual  
284 analysis did not indicate a severe violation of normality. A further exclusion of the non-  
285 significant interaction term removed a former significant effect of particle type. Again, we here  
286 present the more conservative results excluding the interaction term.

287

288 **2 Results**

289 **2.1 Effects on the energy reserves**



290  
 291 Fig. S5: Relative (a) total energy content and (b) total lipid content in the midgut gland (MGG) of *D. polymorpha*  
 292 after an exposure to particle-free medium (Control, 0 p mL<sup>-1</sup>), polystyrene microplastics (MP, 6.4–100,000 p mL<sup>-1</sup>)  
 293 or diatomite (DI, 100,000 p mL<sup>-1</sup>) for 14 d at 14, 23 and 27 °C. Dots = results of each replicate, short lines = mean,  
 294 regression = linear regression of the results in the MP treatment. n = 10 for each temperature and particle  
 295 concentration.

296  
 297 **2.2 Effects of microplastics versus natural particles**

298 Tab. S2: Results of the general linear model and general linear mixed model (only between-subject results)  
 299 analyzing the effects of temperature and particle type (microplastics vs. diatomite) on mussel activity, clearance  
 300 activity (on day 3 and 10), energy reserves (total energy, proteins, glycogen, total lipids) and oxidative stress  
 301 (TBARS, ORAC) in the midgut gland of *D. polymorpha* as well as the phagocytic activity of hemocytes.

302 \* = interaction term not included in the model

303

Variable		Endpoints									
		Mussel activity	Clearance (3 d)	Clearance (10 d)	Total energy	Proteins	Glycogen	Total lipids	TBARS	ORAC	Phagocytic activity
Temperature	df	2	2	2	2	2	2	2	2	2	2
	F	2.165	1.654	5.276	0.839	10.524	7.090	1.027	8.665	8.140	1.337
	p	0.316	0.201	<b>0.008</b>	0.438	<b>&lt; 0.001</b>	<b>0.002</b>	0.365	<b>0.01</b>	<b>0.001</b>	0.280
Particle type	df	1	1	1	1	1	1	1	1	1	1
	F	0.101	3.868	1.221	0.013	3.228	2.279	0.092	0.077	5.688	0.447
	p	0.781	0.054	0.274	0.909	0.078	0.137	0.763	0.782	<b>0.021</b>	0.510
Temperature × Particle type	df	- *	- *	2	2	2	2	2	2	2	2
	F	- *	- *	0.442	0.758	0.628	0.322	0.751	1.523	1.734	0.820
	p	- *	- *	0.645	0.474	0.537	0.726	0.477	0.227	0.186	0.452

304 **3 References**

305 Bradford, M., 1976. A rapid and sensitive method for the quantitation of microgram quantities  
306 of protein utilizing the principle of protein-dye binding. *Anal. Biochem.* 72(1-2), 248-254.  
307 [http://dx.doi.org/10.1016/0003-2697\(76\)90527-3](http://dx.doi.org/10.1016/0003-2697(76)90527-3).

308  
309 Higgs, D. A., Macdonald, J. S., Leving, C. D., Dosanjh, B. S., 1995. Nutrition and Feeding  
310 Habits in Relation to Life History Stage. In: *Physiological physiology of Pacific salmon*, Groot,  
311 C., Margolis, L., Clarke, W. C. (eds), S.189.

312  
313 Jung, M. R., Horgen, F. D., Orski, S. V., Rodriguez, C. V., Beers, K. L., Balazs, G. H., Jones,  
314 T. T., Work, T. M., Brignac, K. C., Royer, S. J., Hyrenbach, K. D., Jensen, B. A., Lynch, J. M.,  
315 2018. Validation of ATR FT-IR to identify polymers of plastic marine debris, including those  
316 ingested by marine organisms. *Mar. Pollut. Bull.* 127, 704-716.  
317 <http://dx.doi.org/10.1016/j.marpolbul.2017.12.061>.

318  
319 OECD, 2016. *Test No. 242: Potamopyrgus antipodarum Reproduction Test*, OECD  
320 Guidelines for the Testing of Chemicals, Section 2, OECD Publishing, Paris.  
321 <http://dx.doi.org/10.1787/9789264264311-en>.